The Use of Thermal Neutron Beams at Medium Power Reactor LWR-15 in Řež for Competetive Neutron Research

P. Mikula and P. Strunz, NPI ASCR, v.v.i. Rez, Czech Rep.

International Conference on Research Reactors: Safe Management and Effective Utilization, Vienna 16-20 November, 2015

Neutron production

Reactor LWR 15, Řež, CZ

- reactor power 10 MW
- thermal flux in the core 1.5 10^{18} $ns^{-1}m^{-2}$
- beam tube 1 10^{13} $ns^{-1}m^{-2}$
- fuel enrichment 36% and 20 % ^{235}U
- tank type
- light water moderated and cooled

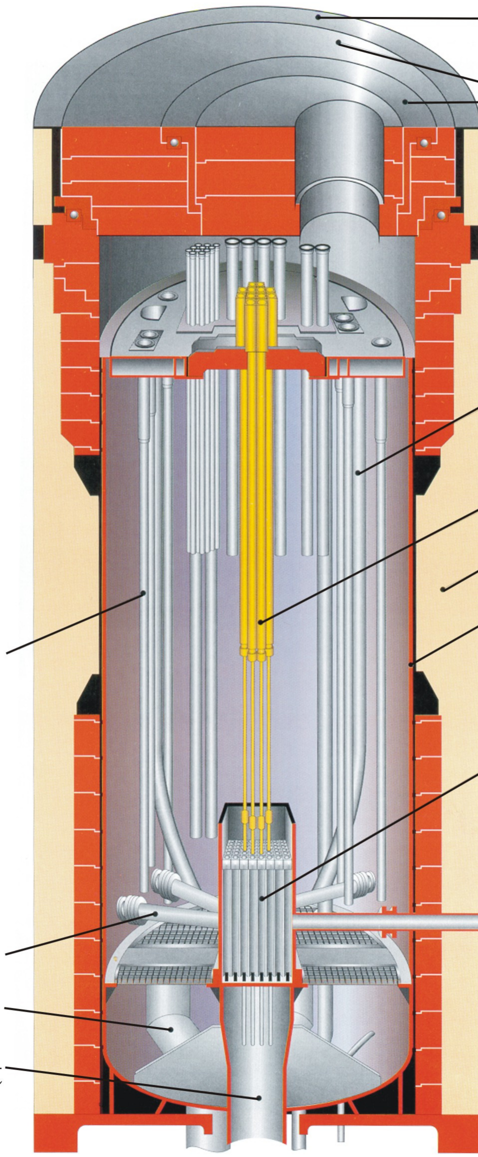

Neutron Physics Laboratory (NPL)

Experimental basis

- horizontal and vertical neutron channels at the research reactor LWR-15 (Research Centre Řež), max. flux 10^{14} n/s/cm^2

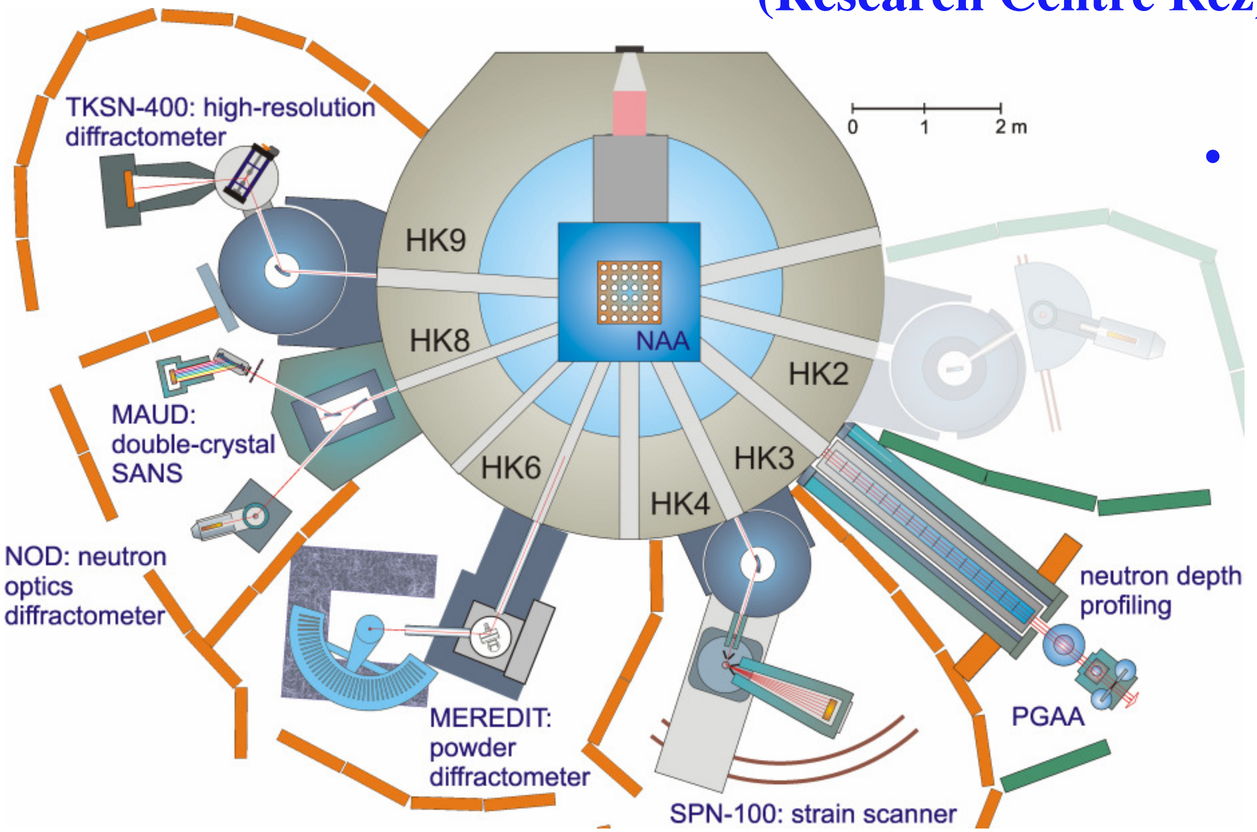

- Access: 8 facilities
  - 3 nuclear-analytical techniques
  - 5 diffraction techniques

- NPL: small lab compared to large neutron-physics centres
  => focus mainly on fields where NPL can be competetive

Reactor parameters

Mean reactor power	10 MW
Maximum thermal neutron flux in the core	$1 \cdot 10^{18}\ n \cdot m^{-2} \cdot s^{-1}$
Maximum fast neutrons flux in the core	$3 \cdot 10^{18}\ n \cdot m^{-2} \cdot s^{-1}$
Maximum thermal flux in reflector (mix of Be + H_2O)	$5 \cdot 10^{17}\ n \cdot m^{-2} \cdot s^{-1}$
Maximum thermal neutron flux in the tubes	$1 \cdot 10^{12}\ n \cdot m^{-2} \cdot s^{-1}$
Maximum thermal flux at the exit of the tubes (100/60 mm)	$1 \cdot 10^{8}\ n \cdot m^{-2} \cdot s^{-1}$
Irradiation channel - in fuel	$1 \cdot 10^{14}\ n \cdot m^{-2} \cdot s^{-1}$
Irradiation channel - at core periphery	$7 \cdot 10^{13}\ n \cdot m^{-2} \cdot s^{-1}$
Doped silicon facility	$1 \cdot 10^{13}\ n \cdot m^{-2} \cdot s^{-1}$
High pressure water loops	$5 \cdot 10^{13}\ n \cdot m^{-2} \cdot s^{-1}$

NPL facilities: Applications (generally):

- materials research using neutron diffraction
- neutron activation analysis, neutron depth profiling
- experiments in nuclear physics

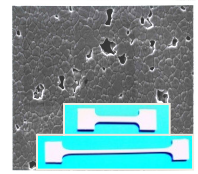

- Advanced metals and ceramics; micro- and macro-strains; structure (incl. magnetic) and microstructure; porosity; in-situ thermo-mechanical processing; phase transformations at high- and low-temperatures; archaeological artifacts.

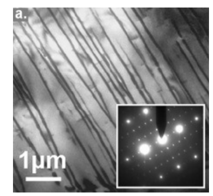

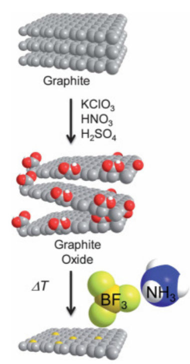

- Non-destructive analysis of concentration profiles of light elements; low-level elemental characterization in biology, biomedicine, environment, geology, metallurgy; prompt gamma activation analysis; nuclear structures.

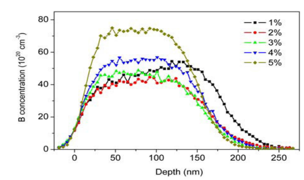

NPL: neutron diffraction facilities

TKSN-400 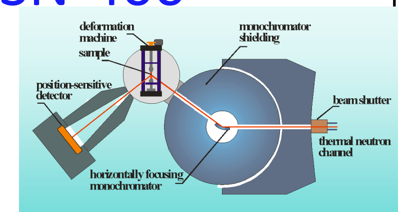	**High-resolution diffractometer**: microstrains in polycrystals, in-situ thermo-mechanical processing, phase transformations in alloys (steels, SMA etc.)
SPN-100 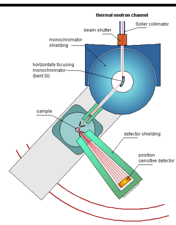	**Diffractometer for macro-strain/stress scanning** of polycrystalline materials (welds, materials after processing)
MAUD 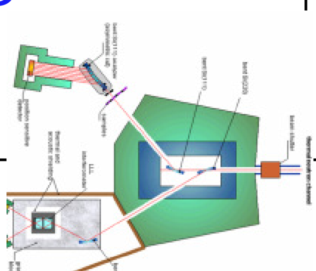	**Double crystal small-angle neutron scattering**: microstructural studies (precipitation in alloys, porosity in ceramics)
NOD	**Neutron optics diffractometer** based on perfect Si crystals for tests of Bragg diffraction optics and imaging
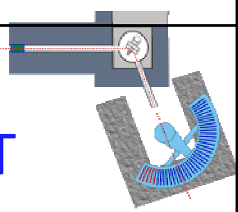 MEREDIT	**Medium resolution powder diffractometer**: standard diffraction experiments; experiments with sophisticated sample environment (T, deformation)

NPL: activation analysis and nuclear physics

<table>
<tr>
<td>T-NDP
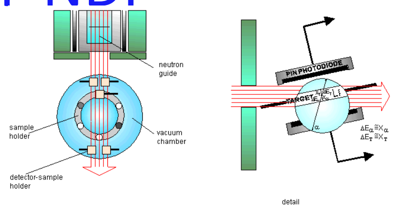</td>
<td>Neutron Depth Profiling:
non-destructive analysis of concentration profiles of light elements (diffusion, sputtering, corrosion, electronics, optronics, life sciences)</td>
</tr>
<tr>
<td>NG
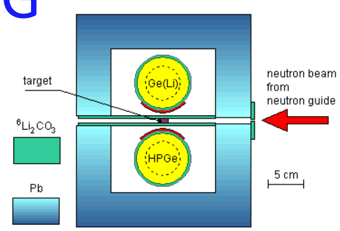</td>
<td>Thermal neutron facility for study of γ-γ coincidences from (n,γ) reactions:
Prompt Gamma Activation Analysis; photon–strength functions, nuclear structure</td>
</tr>
<tr>
<td>NAA
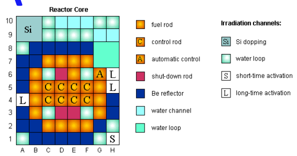</td>
<td>Neutron Activation Analysis:
low-level elemental characterization - biology, biomedicine, environment, geology, archaeometry</td>
</tr>
</table>

MEREDIT: Medium Resolution Powder Diffractometer

- medium resolution 0.4-0.6 %
- automatically exchangeable monochromators (bend Si or Ge or mosaic Cu) provide 5 different neutron wavelengths (1.26, 1.32, 1.46, 1.87 and 1.92 Å)
- **35 individual detectors** with 10' collimators
- diffraction angle 2θ up to 148°

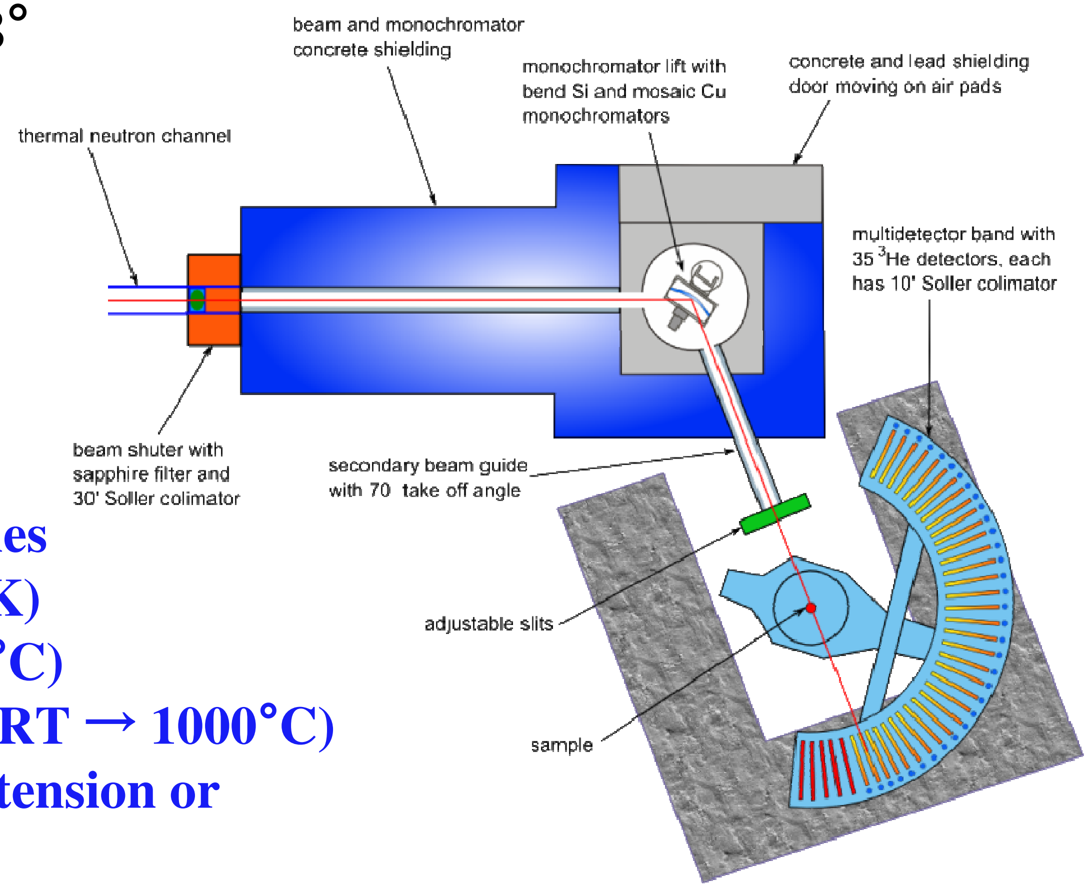

Available sample environment:

- **sample exchanger for 6 samples**
- **close cycle cryostat (RT → 4 K)**
- **vacuum furnace (RT → 1000°C)**
- **light furnace (also gas filling, RT → 1000°C)**
- **deformation rig for uni-axial tension or compression up to 20 kN**

MEREDIT: Medium Resolution Powder Diffractometer

- **instrument status available at http://neutron.ujf.cas.cz/meredit**

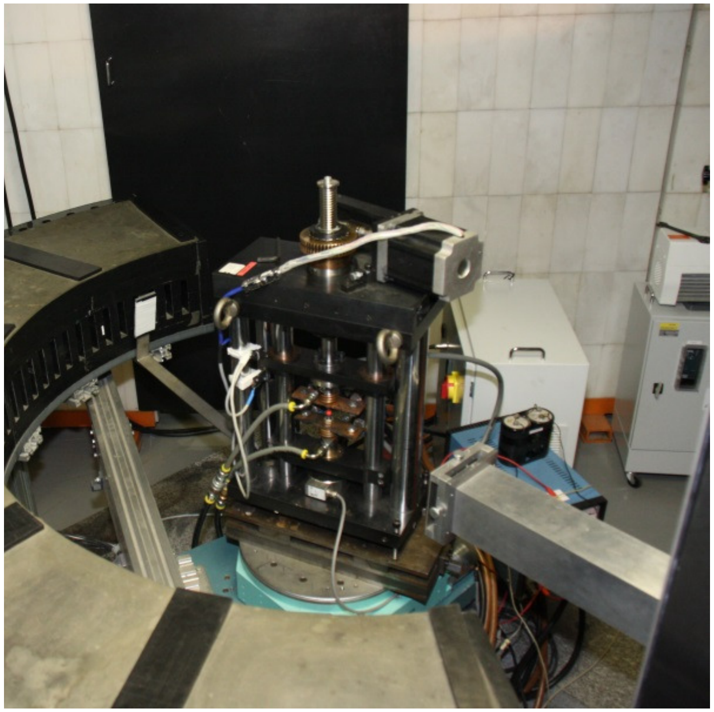

Applications:
- **crystallographic structure characterization, phase analysis**
- **magnetic structure determination and refinement**
- ***in-situ* phase and structure evolution with temperature, stress, etc.**
- ***in-situ* phase and structure evolution in user define sample environment**

MEREDIT – New magnetic ordering in $FeMnP_{0.75}Si_{0.25}$

(Collaboration with Dept. of Materials, Uppsala University, Sweden)

- **detailed study of magnetic ordering in $FeMnP_{0.75}Si_{0.25}$**

- **Candidate for magnetic refrigeration material**
- **Magnetocaloric effect sensitive to P and Si ratio**

- **Structure refinement at**
- **RT → non-magnetic, hexagonal Fe_2P-type structure**

- **Determination of ordering or disordering on Fe/Mn crystallographic sites → 97% ordered Fe/Mn on individual sites**

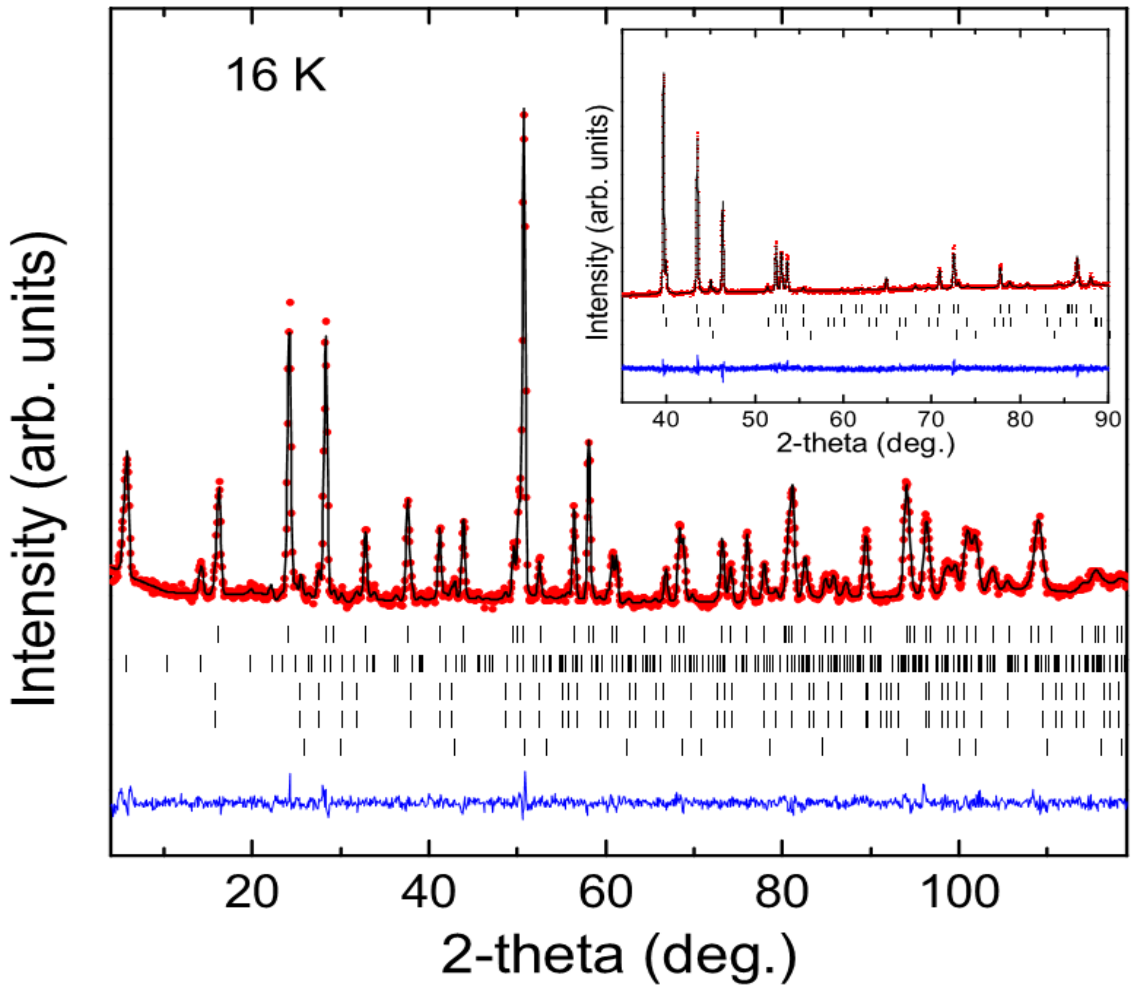

MEREDIT – New magnetic ordering in $FeMnP_{0.75}Si_{0.25}$

- **investigation and determination of the magnetic structure at 16 K → incommensurate anti-ferromagnetic structure with propagation vector q_y=0.36**

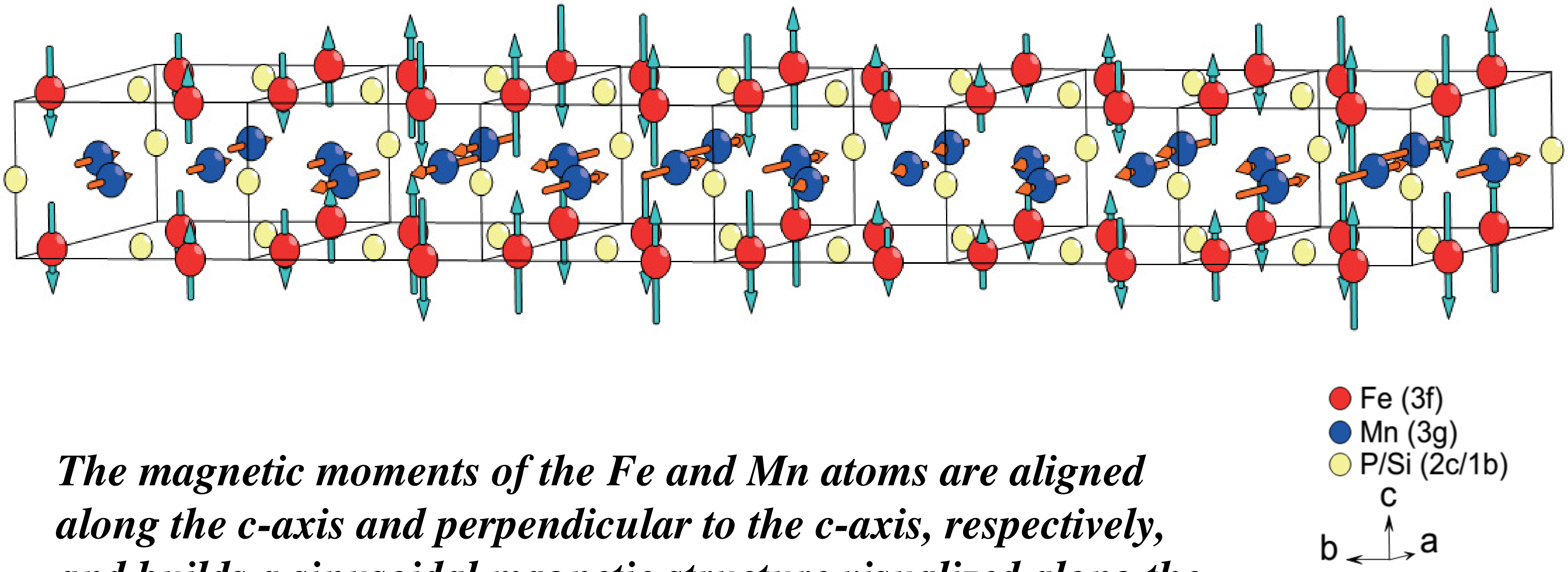

The magnetic moments of the Fe and Mn atoms are aligned along the c-axis and perpendicular to the c-axis, respectively, and builds a sinusoidal magnetic structure visualized along the b-axis.

TNDP - Thermal Neutron Depth Profiling

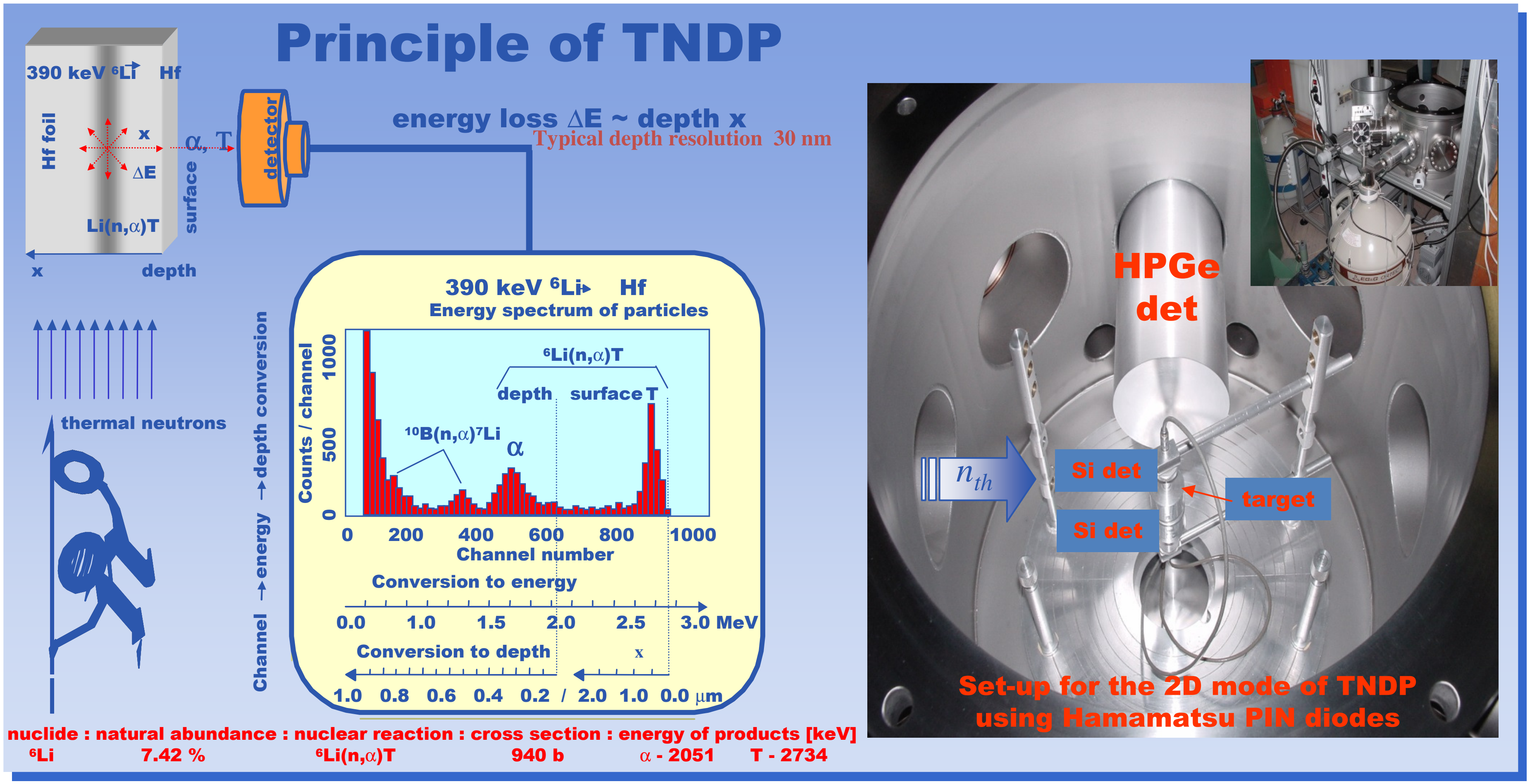

Non-destructive technique for measurement of concentrations versus depth distributions in the near-surface region of solids. TNDP utilizes thermal neutron induced reactions (n_{th},p) or (n_{th},α) on certain light isotopes (^{3}He, ^{6}Li, ^{7}Be, ^{10}B, ^{14}N, etc.) in 1D or 2D modes, analyzing elements in depths up to tens of μm with a nominal depth resolution ≈10 nm.

Separation of the intra- and intergranular magnetotransport properties in nanocrystalline diamond films on the metallic side of the metal-insulator transition

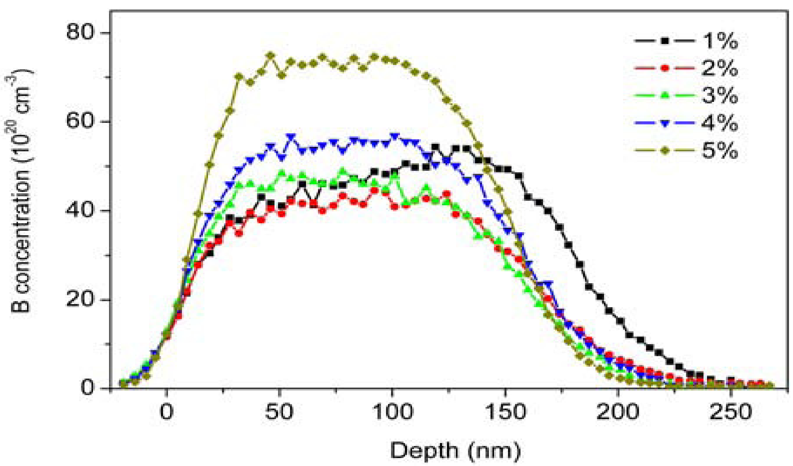

The meutron depth profiling of B for the NCD layers.

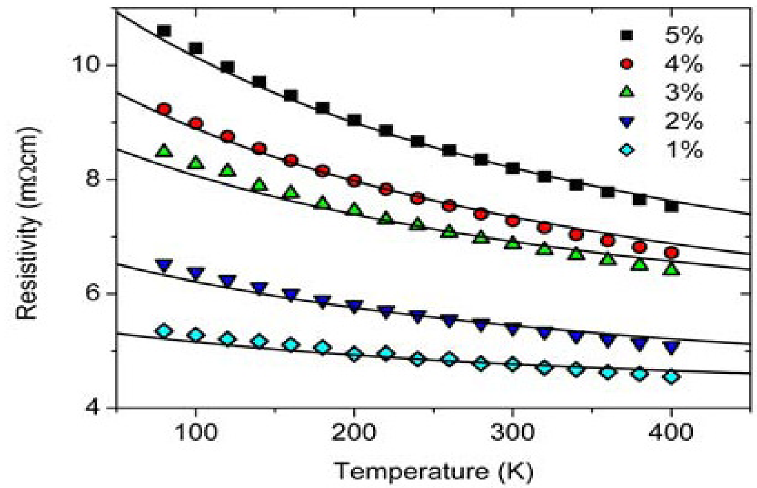

The resistivity as a function of temperature for different C/H-ratio.

General aim:

electronic properties of heavilly B-doped nanocrystalline diamond (B:NCD) thin films (~150 nm), grown with a fixed B/C-ratio (~5000 ppm), but with various C/H-ratios (1 - 5%)

Result TNDP:

•lower B-incorporation for B:NCD grown with lower C/H-ratio, confirmed by TNDP

•=> the concentration of active charge carriers reduced (see resistivity)

SPN-100: Diffractometer for macrostrain scanning

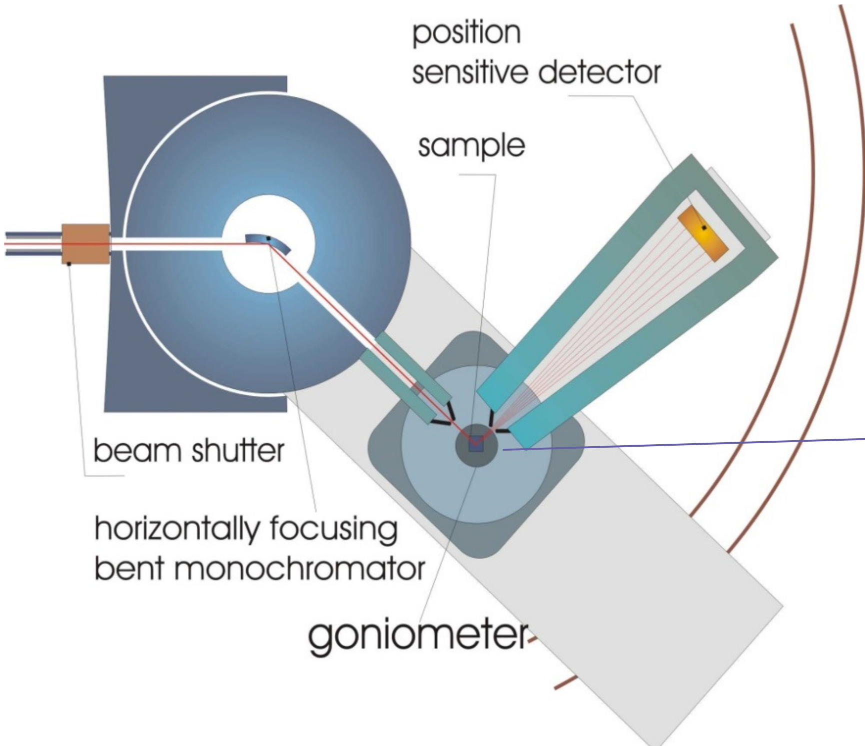

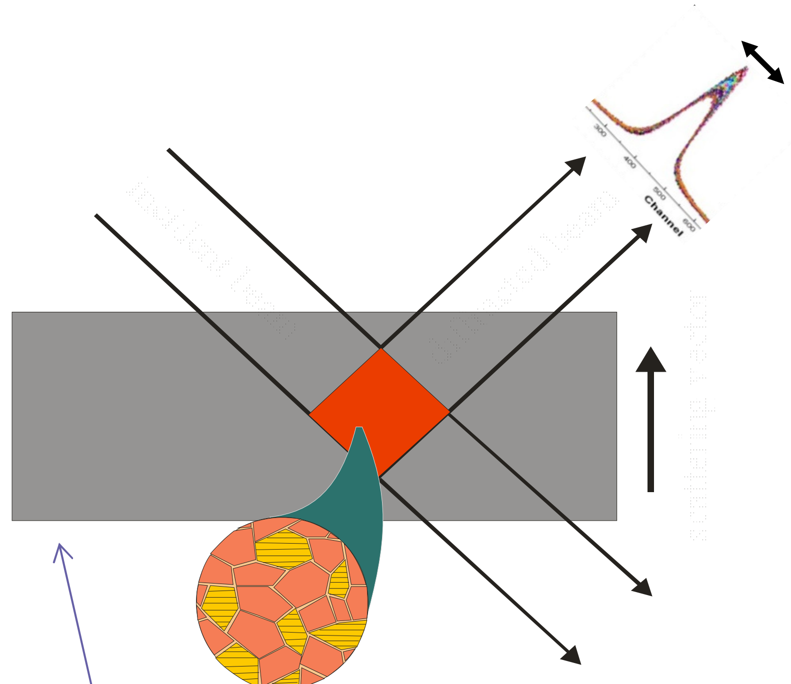

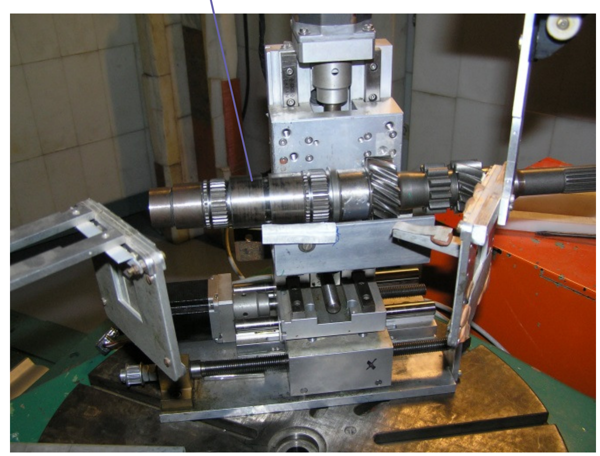

Application:

Residual stress determination:

- **around welds**
- **in metals after processing**
- **in ceramics (e.g. functionally graded Al_2O_3/Y-ZrO_2)**

Neutron diffraction scanning of residual stresses and their effect on fatigue strength of high-strenght steels welds

- **Collaboration with the Welding Research Institute, Bratislava, Slovakia and ESAB AB, Goetenburg, Sweden**

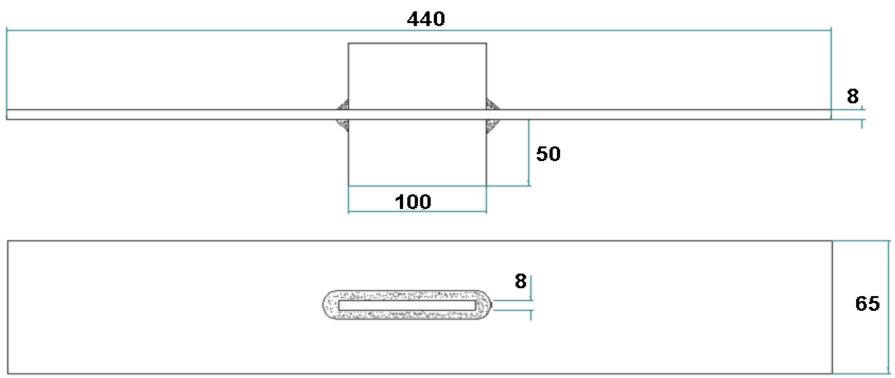

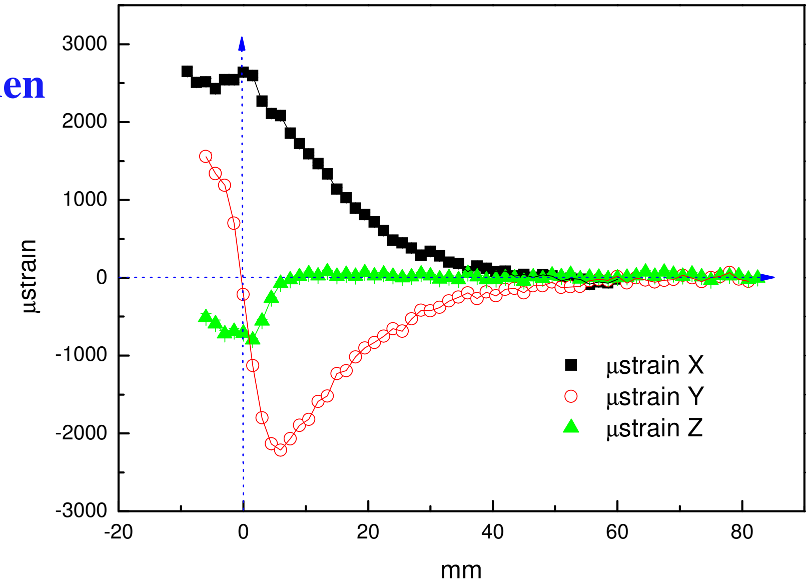

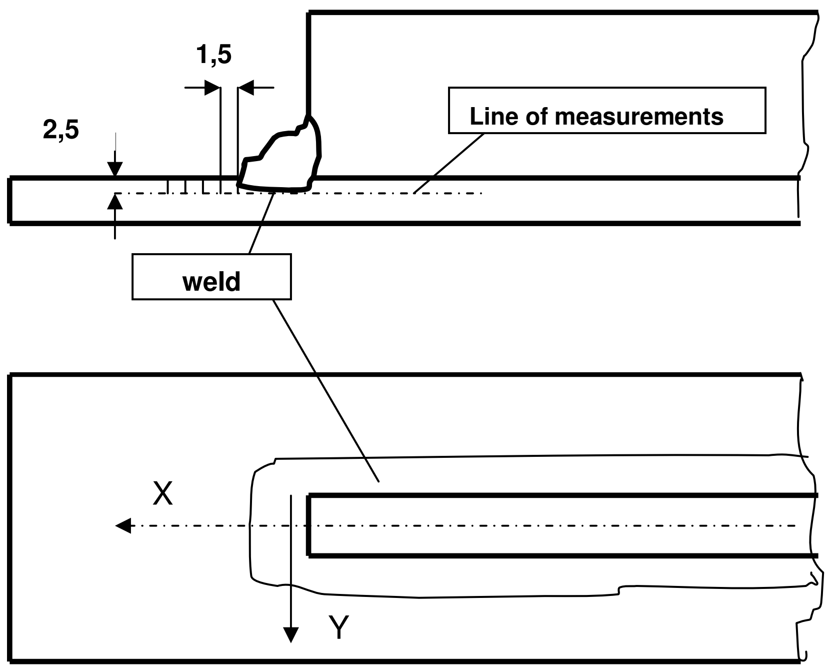

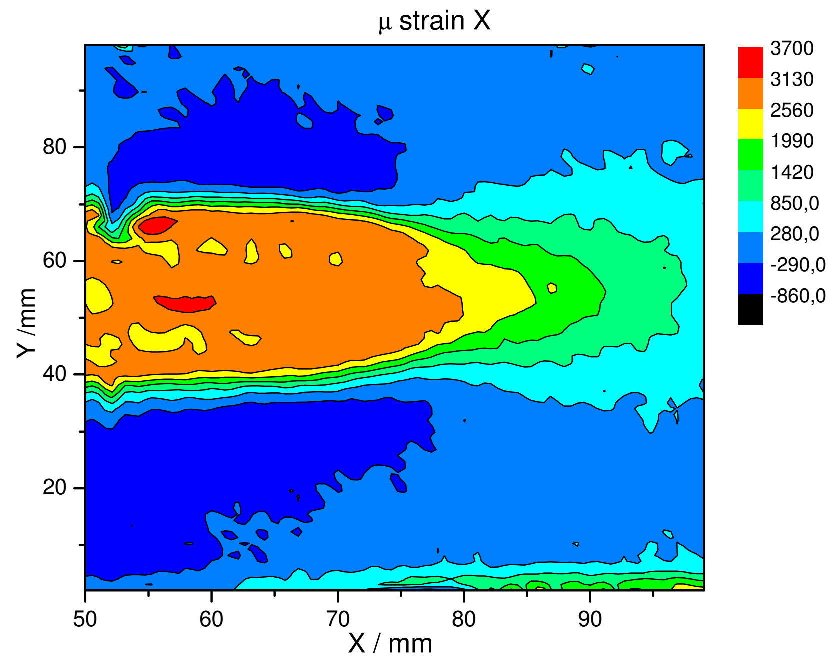

Residual stresses of high-strenght steels welds - The effect of filler materials

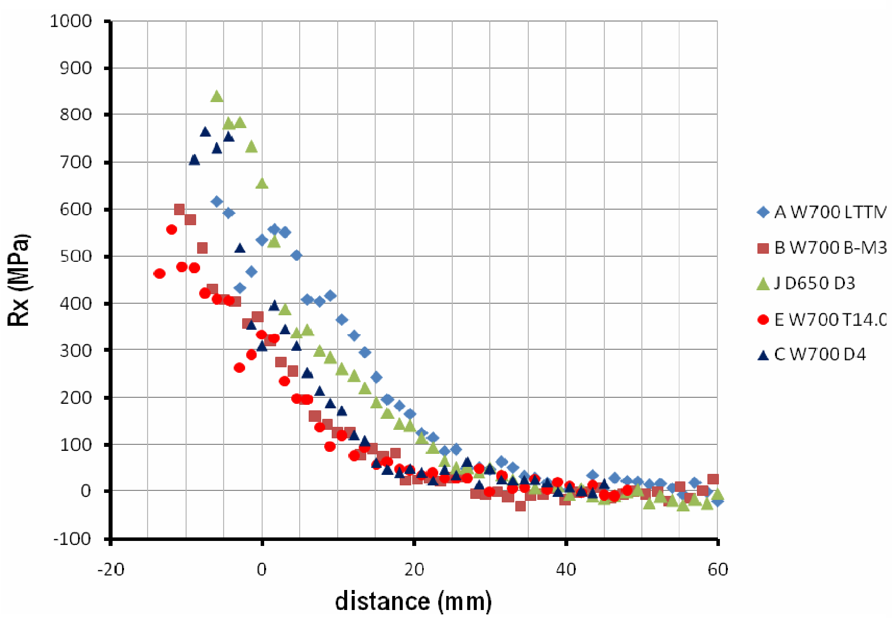

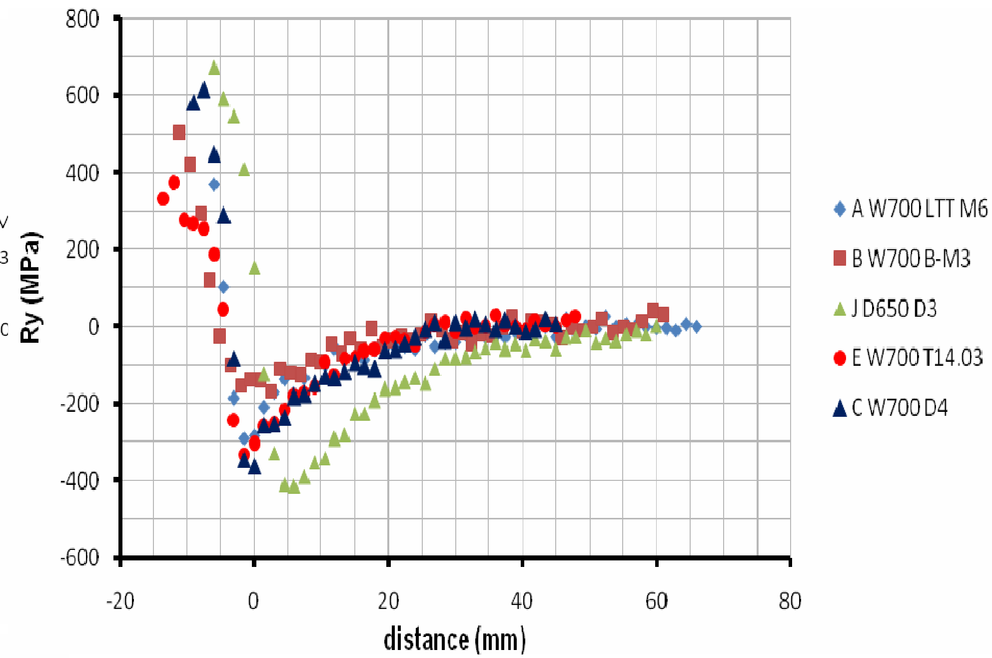

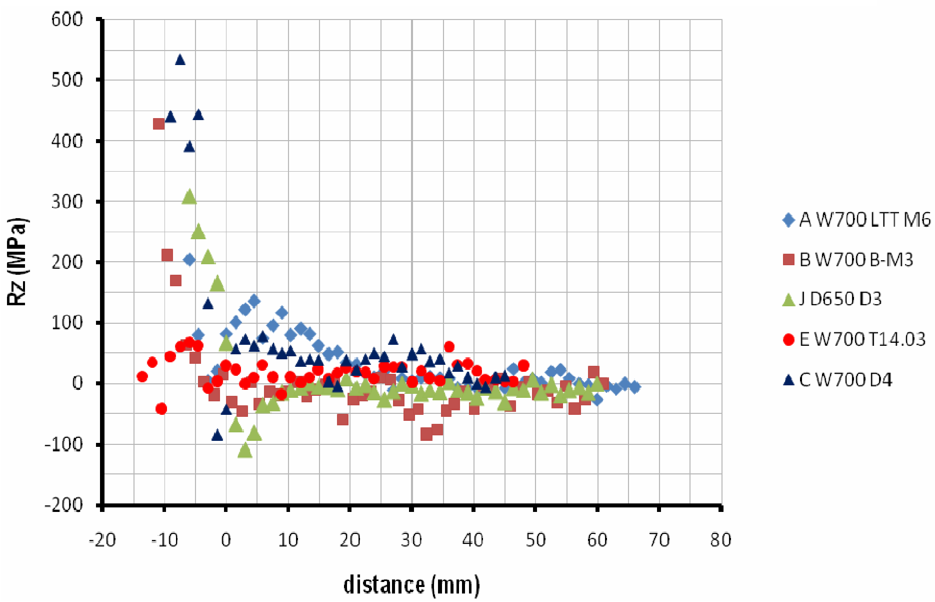

The effect of filler material

Residual stress distribution in the vicinity of the WELDOX 700/690QL fillet test welds welded by various filler materials: A - LTT-M6,
B - B-M3,
C – D4-6547,
E - Tubrod 14.03,
J - D3-5724

TKSN-400: high-resolution diffractometer

Angular range 25° < 2θ < 90°
Resolution $2\times10^{-3} \leq \Delta d/d \leq 3\times10^{-3}$

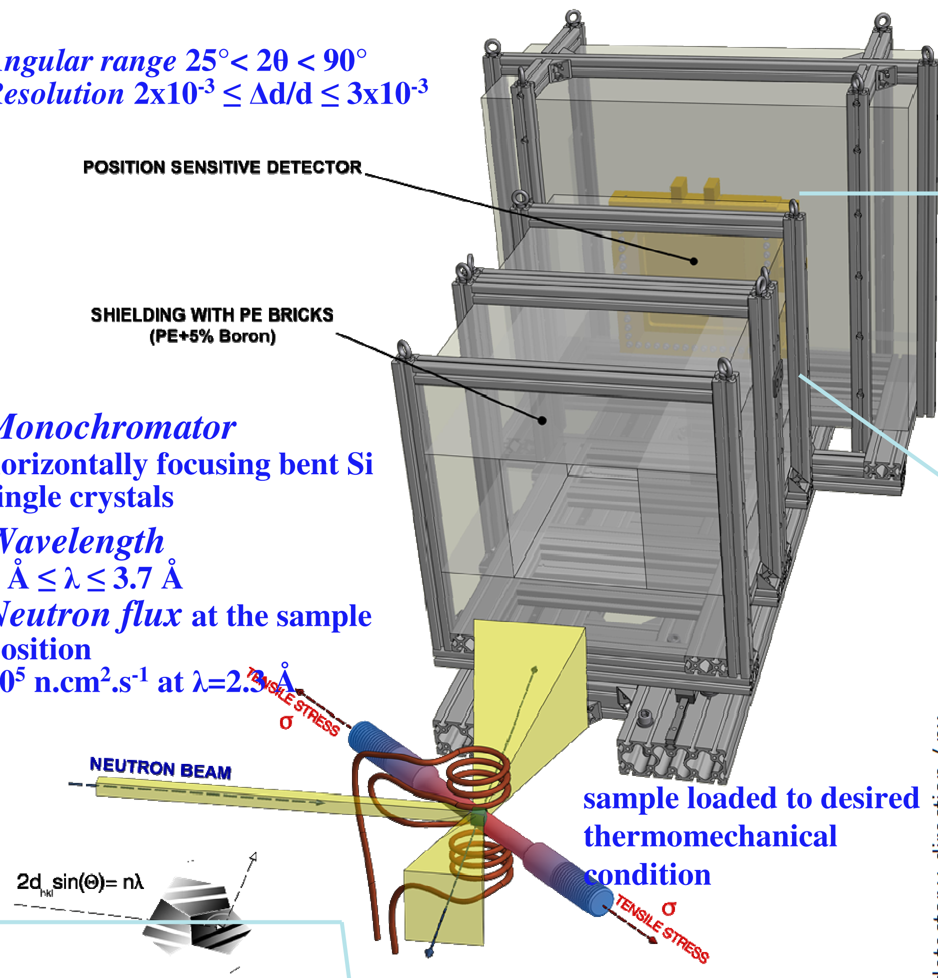

Monochromator
horizontally focusing bent Si single crystals

Wavelength
1 Å ≤ λ ≤ 3.7 Å

Neutron flux at the sample position
10^5 n.cm^2.s^{-1} at λ=2.3 Å

- optimized for investigation of microstrains in polycrystals under thermomechanical load
- recently: complete upgrade

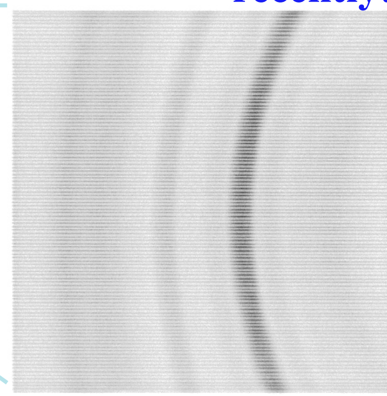

Example of the 2D image taken by the new neutron detector

sample loaded to desired thermomechanical condition

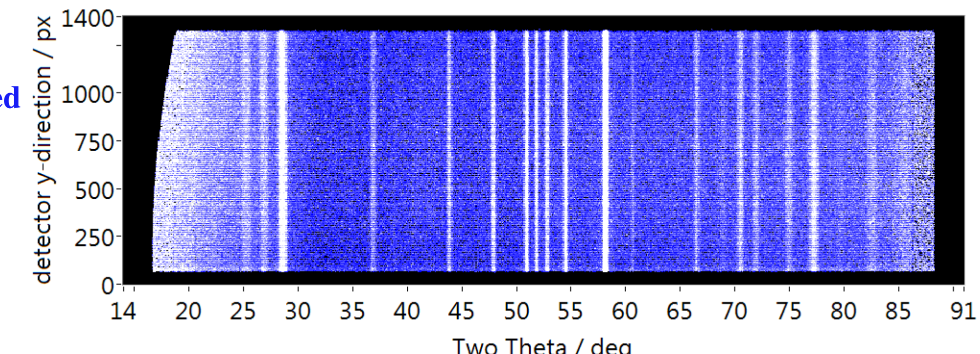

Full 2D image for high resolution Mg diffractogram of Mg reconstructed from twenty individual 2D images (detector at various 2θ)

Sample environments:
Deformation rig (uni-axial loading) ± *20 kN*,
resistivity heating (T < 1200° C)
Hot-air heating (T < 300° C)
Miniature deformation rig for uni-axial loading ± 10 kN
Eulerian cradle: inner diameter of 400 mm, 0° < χ < 160°, 0° < φ < 360°
Deformation rig for bending loading, max. cycling frequency of 27 Hz

Investigation of deformation mechanisms taking place during mechanical loading of magnesium samples

(Collaboration with Charles University Prague)

- **Hexagonal Magnesium with 1% of zirconia (used for grain boundary stabilization)**
- **the aim: to understand basic deformation mechanisms during thermomech. loading**
- **diffraction peaks measured in-situ during compression and tension loading**

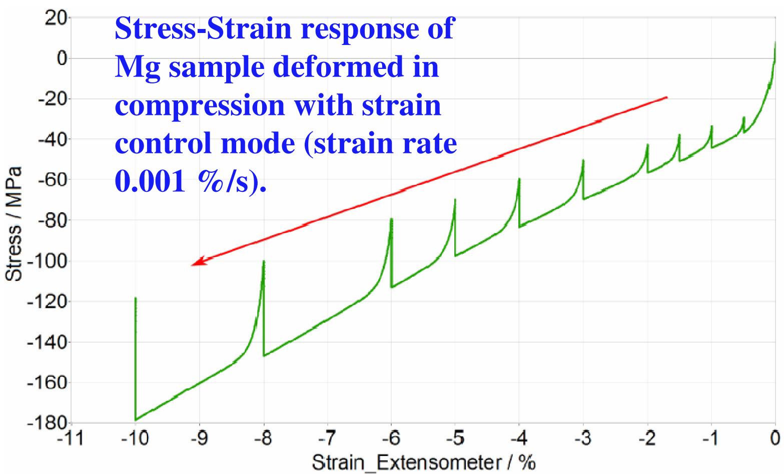

Stress-Strain response of Mg sample deformed in compression with strain control mode (strain rate 0.001 %/s).

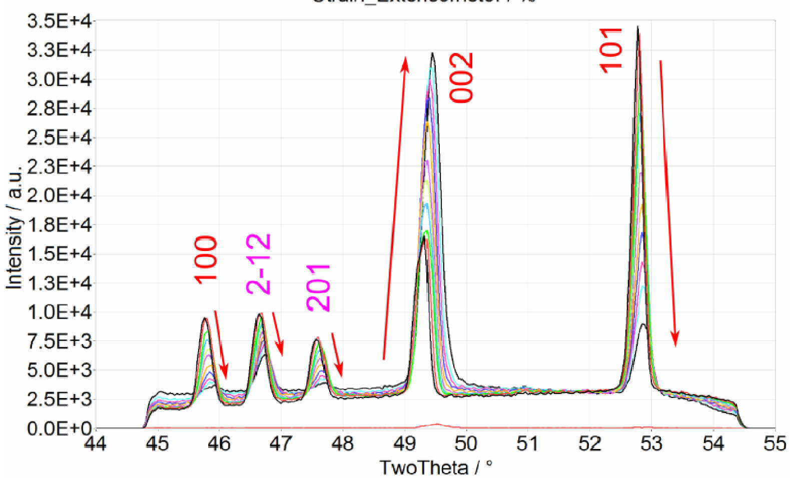

The most active twinning mechanism in Mg and its alloys: {10.2} twinning plane --> reorientations of a parent *hk.l* grains by 86.3°.
Accompanied by characteristic changes of integrated intensities of particular *hk.l* diffraction peaks i.e. {10.1} -> {00.2} .

=> Quantitative characterization of twining process and stress relaxation

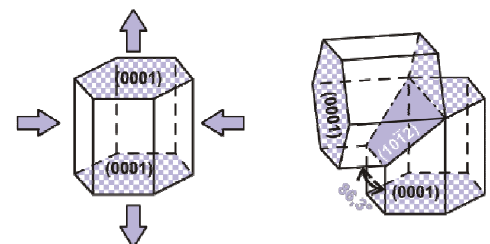

- **5 reflections represented lattice planes perpendicular to the loading direction under various loading strains.**
- **Stress relaxations during diffraction measurements (4 hours each point) are clearly evident on stress-strain curve.**

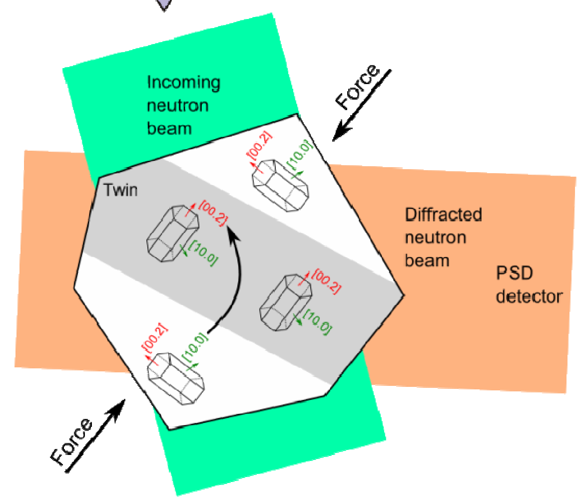

MAUD: high-resolution small-angle scattering instrument

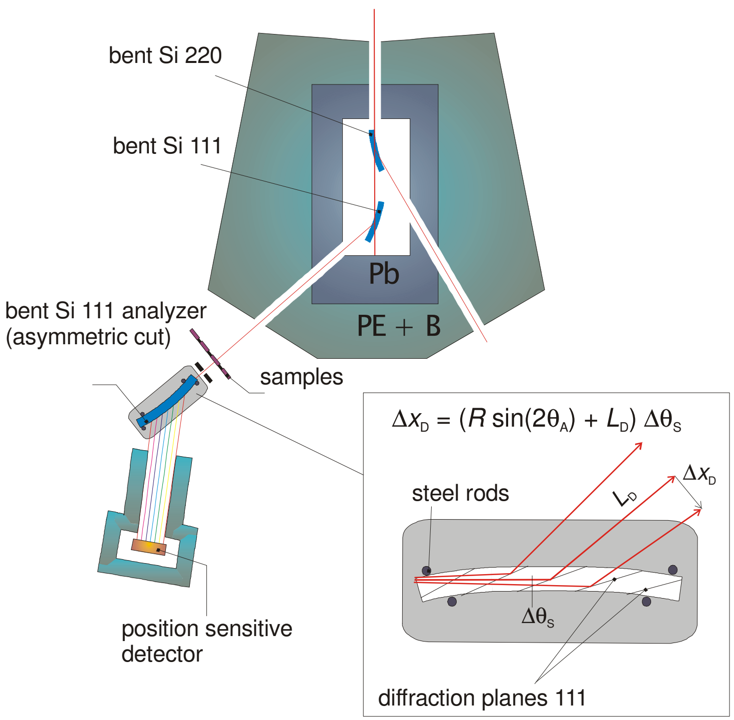

Monochromator	**bent perfect crystal Si(111), symmetric dif. geometry**
Sample	**Max. irradiated cross-section $4x25\ mm^2$**
Analyzer	**bent perfect crystal Si(111) fully asymmetric geometry**
Detector	**1 and 2-dimensional ^3He PSD Spatial resolution ~ 1.5 mm**
Wavelength	**2.09 Ă**
Neutron flux	**$5 \cdot 10^3 \div 5 \cdot 10^4\ n \cdot s^{-1} \cdot cm^{-2}$**
Q-resolution	**$10^{-4} \div 10^{-3}$ Ă$^{-1}$**
Q-range	**$2 \cdot 10^{-4} \div 2 \cdot 10^{-2}$ Ă$^{-1}$**
Size range	**500 Ă ÷ 2 μm**

Sample environment:

- **Sample changer**
- **Sample changer with thermoregulation 25÷120°C**
- **transmission vacuum furnace (RT → 1400°C)**
- **Horizontal magnet up to 2 T**
- **deformation rig for uniaxial tension or compression up to 20 kN**

MAUD - Applications

Examples:

- Precipitates in Ni-based or CoRe-based superalloys
- Porosity, cavitation and cracks in ceramic materials (EB-PVD zirconia-based turbine blade coatings(TBC), superplastically deformed Y-TZP, plasma-spayed Al_2O_3)
- Mixtures of partially solvable liquids stabilized by di-block copolymer
- Degradations in turbine blades
- Morphology of new type zirconia-based glasses
- Porous silica particles

MAUD – Inner structure of large sintered artificial opals

(Collaboration with Petersburg Nuclear Physics Institute, Russia)

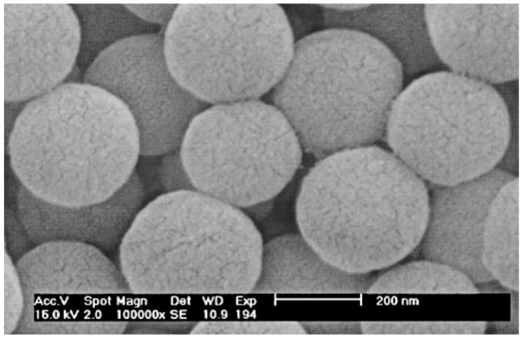

- mesoporous silica (SiO_2)
- synthesis by surfactant-templated method

  Application:
- photonic glasses and photonic crystals used in nanophotonics and optoelectronics (e.g. random lasers, fluorescence emitters and optical filters)
- chemo-mechanical polishing
- porous ferromagnetic composite

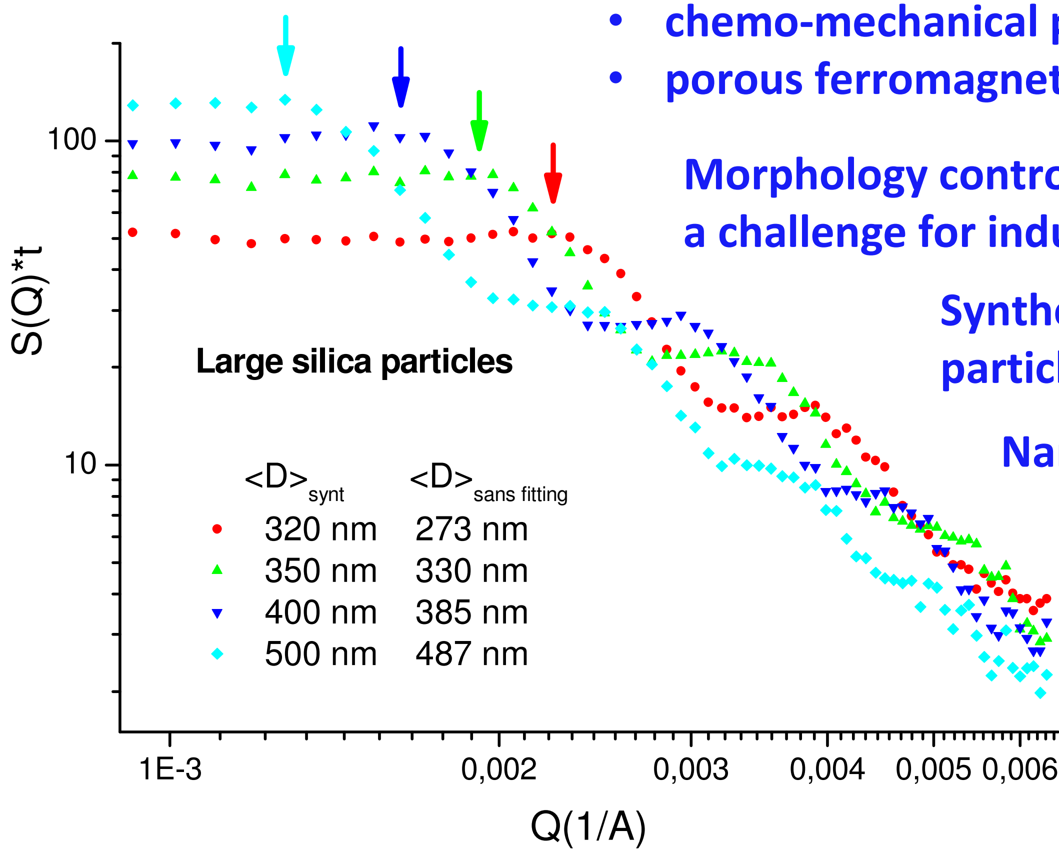

Morphology control (fiber, film-like, polyhedral, spherical) – a challenge for industrial use of mesoporous silica

Synthesis of spherical particles with uniform particle size - essential for some applications

Nanochannels 2-10 nm – pin-hole SANS

Complementary DBC SANS: to complement the characterization: secondary particles presence (60 nm), morphology, homogeneity of particles, size uniformity

NOD: Neutron Optics Diffractometer

- bent Si(111) premonochromator, fixed neutron wavelength of 0.162 nm
- two or three axis mode + goniometer
- neutron detection:
  - point detector
  - linear position sensitive detector (spatial resolution of 2 mm)
  - FUJI imaging plate with the resolution of 50 µm x 50 µm

Applications

•primarily designed for testing neutron diffraction optics elements (neutron monochromators and analyzers)
•high and ultrahigh resolution neutron monochromators based on multiple reflections in bent perfect Si and Ge
•focusing properties of dispersive double-bent crystal arrangements
•can be used for neutron texture measurements

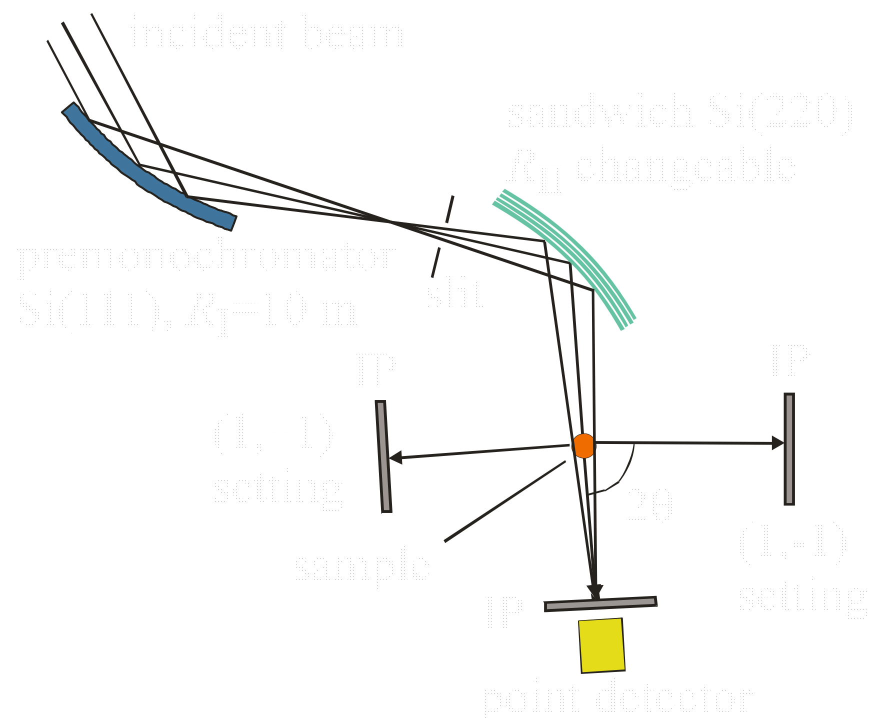

Quasiparallel beam diffracted by a sample

R_1

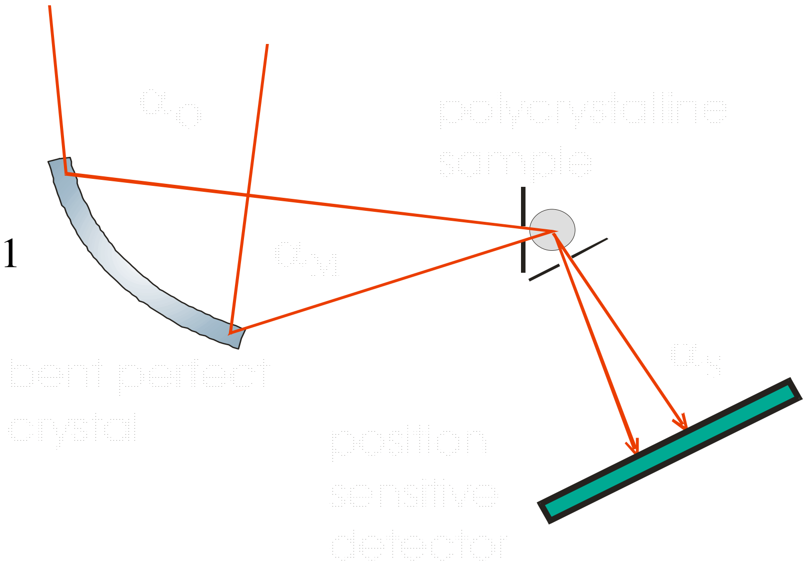

R_3

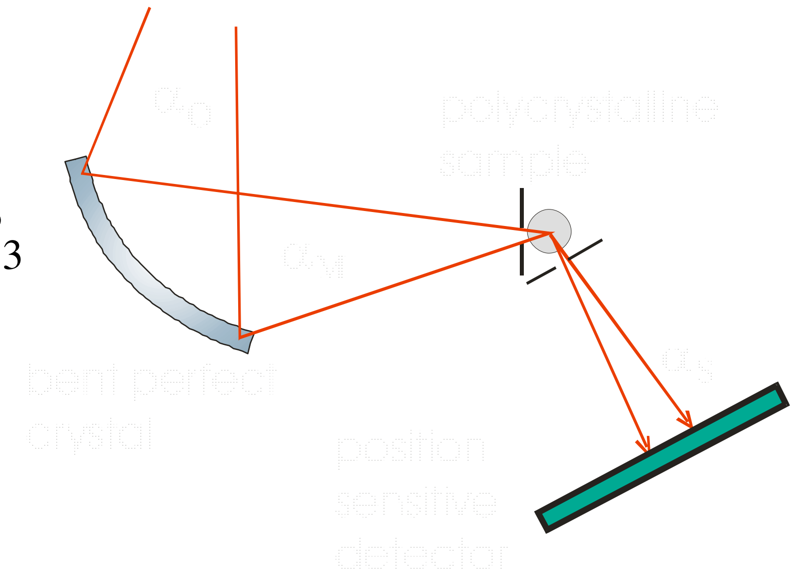

$R_1 > R_2 > R_3$ R_2 - optimum

R_2

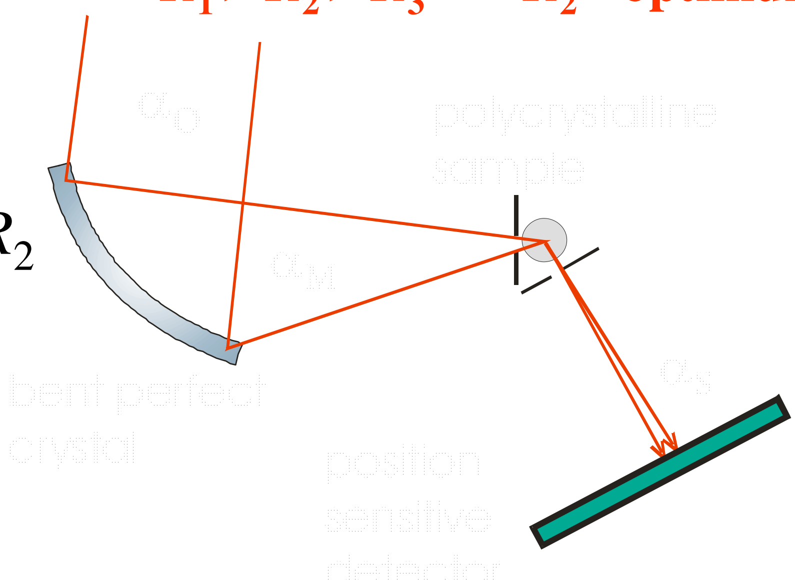

$\Delta\theta_2 = \Delta\theta_1\,[2\,(\tan\theta_S / \tan\theta_M)(1 - L_{MS}/2f_M) - 1]$

can be manipulated through R_M. For

$R_M = (2L_{MS}/\sin(\theta_M - \varphi))/(2 - 1/a_{SM}) \;\rightarrow\; \Delta\theta_2 = 0$

parallel diffracted beam

Free parameters: Radius of curvature R, monochromator-sample distance L_{MS}, monochromator take-off angle $2\theta_M$, scattering angle $2\theta_S$

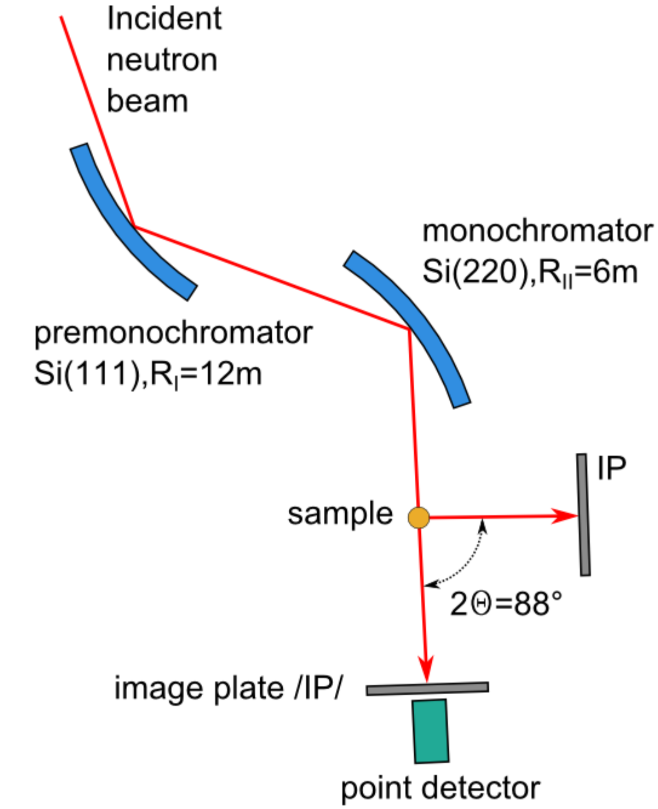

Schematic layout of the diffractometer permitting experiments in two or three axis mode.

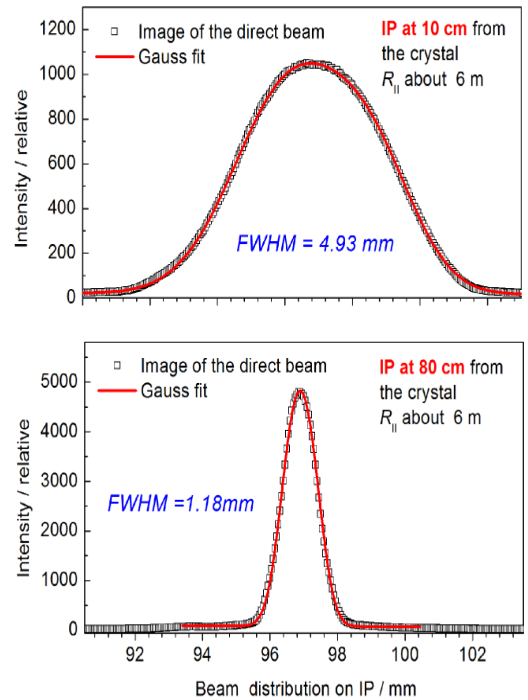

Profiles of the beam as taken by IP at 10 cm and 80 cm distance from the second crystal for R_{II}=6 m provide an evidence of a strong real space focusing.

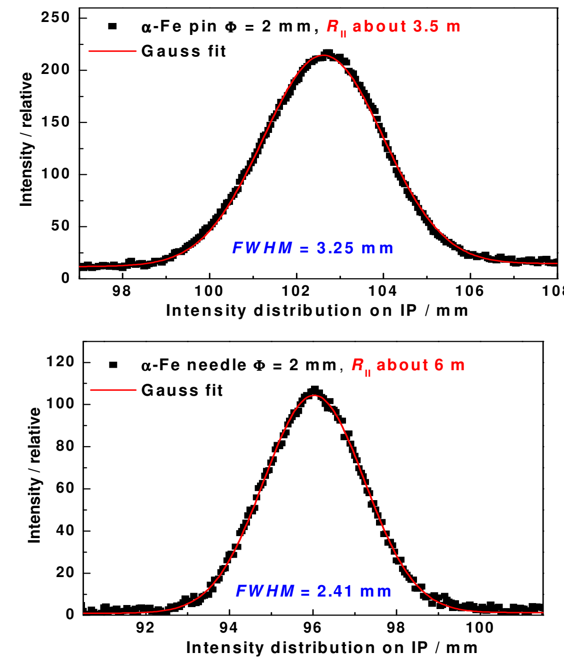

Diffraction profiles of the beam as taken by IP from the α-Fe(211) polycrystalline sample situated at 50 cm from the Si(220) crystal and with IP at 45 cm from the sample for two different curvatures.

Neutron activation analysis (NAA) at vertical channels of the LVR-15 experimental reactor

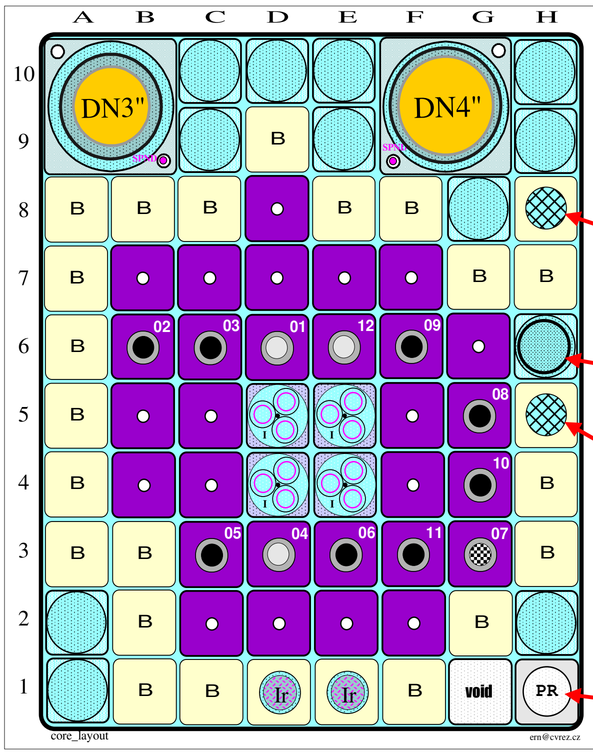

H8 - long-time irradiation

H6 - long-time irradiation

H5 - long-time irradiation

H1 - short-time irradiation with pneumatic facility (transport time ~ 3.5 s)

Example of active core configuration

fuel

beryllium

facility for Si dopping

facility for U irradiation

facility for Ir irradiation

channels for NAA irradiation

Neutron fluence rates of up to $5 \cdot 10^{13}$ cm^{-1} s^{-1} are available in vertical channels H1, H5, H6, H8. Epicadmium irradiation possible in channels H1 and H6.

Facilities for γ-ray spectrometry

- Four coaxial HPGe detectors with rel. efficiency 21-78 %, FWHM resolution 1.75-1.85 keV at 1332.5 keV
- Two planar HPGe detectors, effective area of 500 mm^2, thickness of 15 mm, FWHM resolution of 550 eV at 122 keV
- One well-type HPGe detector with the active volume of 150 cm^3, FWHM resolution of 2.02 keV at 1332.5 keV, well dimensions 16x50 mm
- The detectors are coupled to a Canberra Genie 2000 γ-spectrometric system
- Two coaxial HPGe detectors are equipped with a pneumatic sample changer

NAA standardization and modes

- Both relative and k_0 standardization using KAYZERO for Windows and k0-IAEA software available
- Using both short-time (10 s - 3 min.) and long-time (several hours - several days) irradiations, information about concentrations of up to 65 elements can be obtained, in many cases by non-destructive, so-called instrumental neutron activation analysis – **INAA** with detection limits shown in Fig. 2.
- Epithermal instrumental neutron activation analysis – **EINAA** yields improvement of detection limits for selected elements up to one order of magnitude compared with INAA
- Procedures for radiochemical neutron activation analysis – **RNAA** are available for the elements V, Cr, Co, Ni, Cu, As, Se, Mo, Sb, I, rare earth elements, Re, and Hg that yield detection limits down to the ng g^{-1} level

INAA limits of detection (LOD)

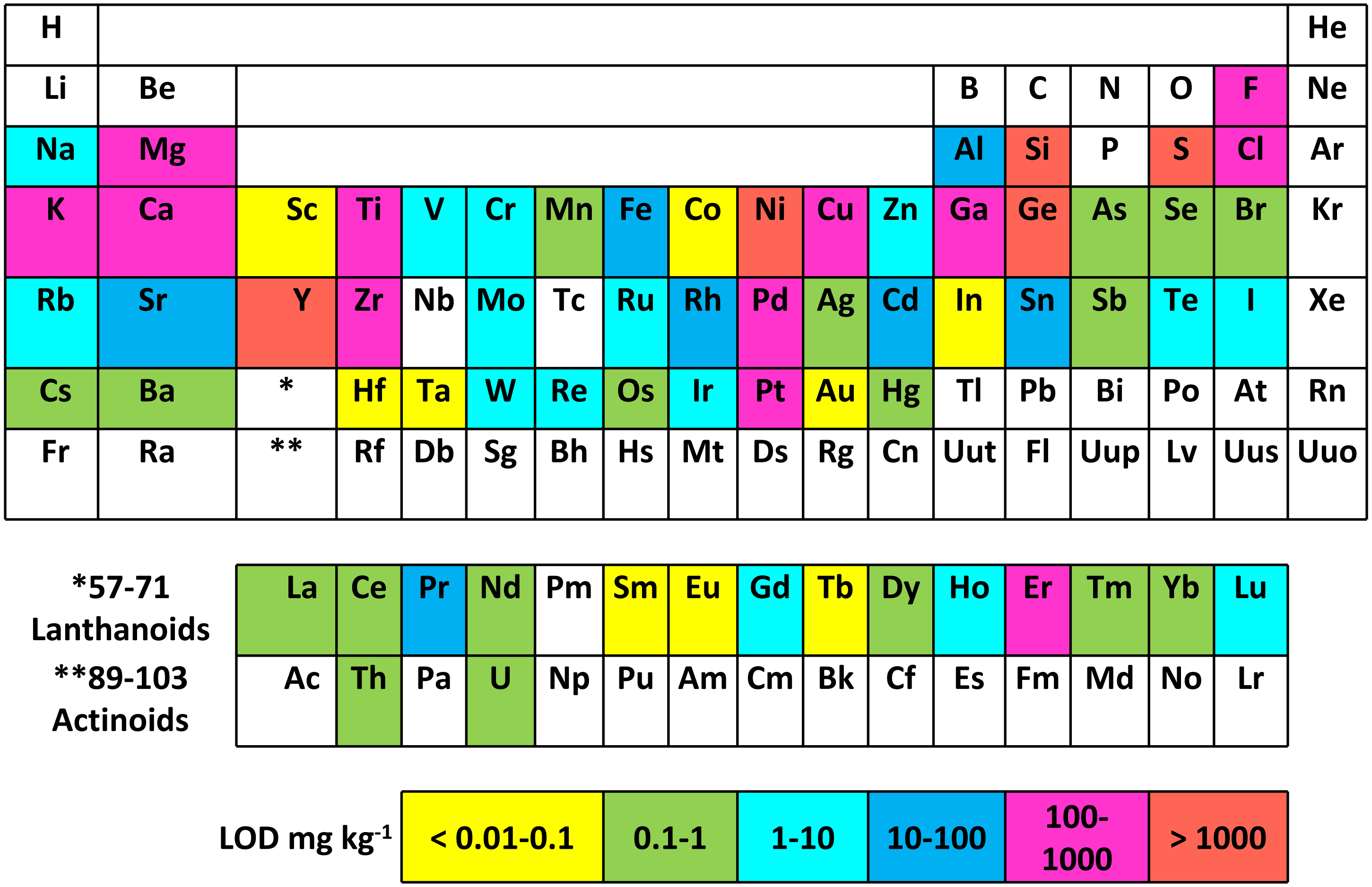

INAA limits of detection for 150-mg soil samples

NAA of remains of Tycho Brahe (1546-1601)

After re-opening of the Tycho Brahe´s tomb in Prague in 2010 by a Czech-Danish consortium, samples of hair and bones were procured and analyzed by NAA and µ-PIXE in Řež and by AAS in Odense to find out whether the world renowned astronomer was poisoned by mercury as it was rumoured.

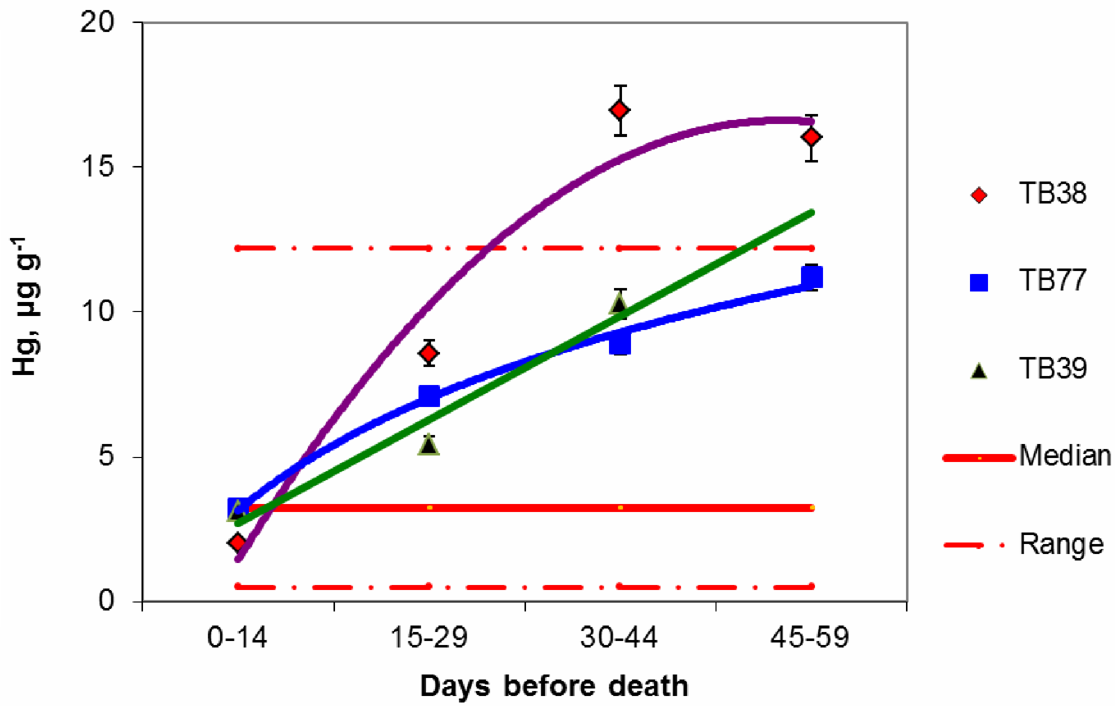

Determination of Hg by RNAA of 5-mm hair segments proved that accute exposure (poisoning) of Tycho Brahe can be excluded and determination of Hg by AAS and RNAA in bones proved that long-term Hg exposure can be excluded, as well.

K. L. Rasmussen, J. Kučera, L. Skytte, J. Kameník, V. Havránek, et al., Archaeometry, 2012, doi: 10.1111/j.1475-4754.2012.00729.x

2. Selenium determination in cereal plants and cultivation soils by RNAA

A Se fortification study carried out in co-operation with Technical University of Lisbon, Instituto Tecnológico e Nuclear, Sacavém, National Institute of Biological Resources. Se contents as low as 3 ng g^{-1} determined.

C. Galinha, M. C. Freitas, A. M. G. Pacheco, J. Kameník, J. Kučera et al. J. Radioanal. Nucl. Chem., 294 (2012) 349–354

3. Elemental characterization of nanocarbon particles prepared by various processes by k_0-INAA

A co-operation with the Institute of Chemical Technology in Prague. To be published.

4. Elemental characterization of a candidate reference material of Single-wall carbon nanotubes by INAA and k_0-INAA

A co-operation with ANSTO, Australia, National Research Council Canada, U.S. A co-operation with National Institute of Standards and Technology, CENA, USP, Brazil. To be published.

5. Determination of K, Th and U in bricks by INAA and EINAA for the assessment of the annual dose for luminescence dating

A co-operation with the Czech Technical University in Prague.
Rad. Phys. Chem., submitted.

6. Determination of Si in beer and semiproducts of beer brewing by INAA with fast neutrons

A study on the impact of the brewing process on the concentration of silicon in lager beer in co-operation with the Institute of Chemical Technology in Prague.

J. Inst. Brewing, submitted.

7. Interlaboratory Comparison of NAA laboratories organized by the IAEA Vienna (project RER 1/007).

Evaluation of performance of NAA laboratories from 12 countries. IAEA TECDOC to be published.

NG: γ–γ coincidence facility

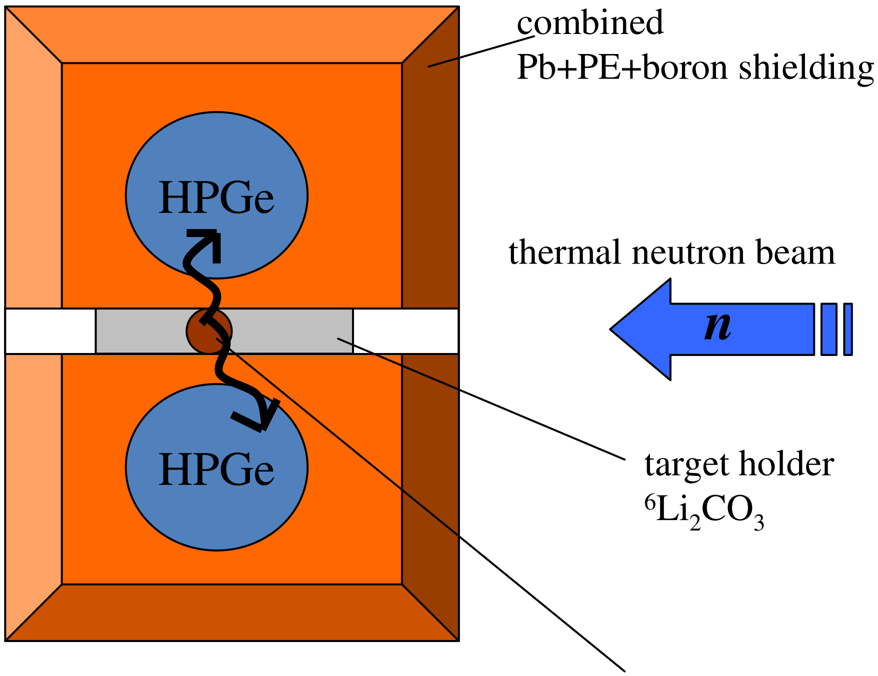

Instrument parameters

Neutron flux : $3x10^6$ n/cm^{2}s
(Cd ratio about 10^5)
Beam shape (cross section) : 20x2 mm^2
γdetection: two HPGe detectors - about 25% rel. eff. , shielded by $^6Li_2CO_3$
Electronics equipment: fast/slow coincidence electronic system
Coincidence efficiency: about $5x10^{-5}$ for cascade from ^{60}Co rad. source
Output data format: event-by-event

Application:

- **study of Photon Strength Functions (PSF) via a (n,γγ) reaction and using Two-Step Cascade (TSC) method (statistical properties of nucleus – γ decay)**
- **nuclear spectroscopy via a (n,γγ) reaction (level and decay schemes, nuclear structure studies)**

NG: PGAA facility

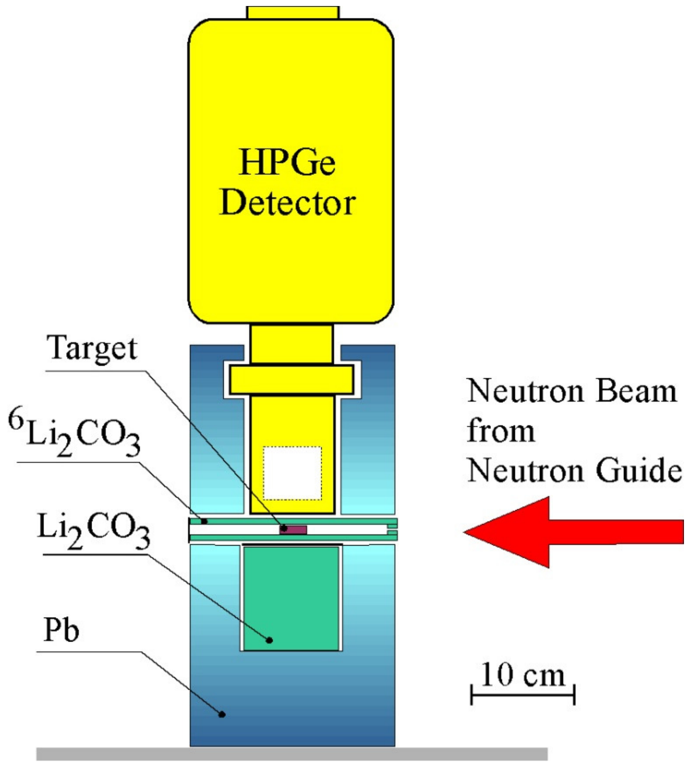

Application: Nuclear analytical method
- concentration of isotopes/elements (B, Cd, Sm, Gd, H, Cl, ...)
- optimized for liquid (powder) samples

Instrument parameters

Neutron flux $3x10^6$ n $cm^{-2}s^{-1}$

Beam $25x7$ mm^2

Detector HPGe (25%)

Sensitivity 3.7 counts/s /µg ^{10}B

Sample packaging 0.5 ml Teflon vial

Capability: 1 ppm of ^{10}B in 0.5 ml with stat. err. 5% within 25 minutes

Measurement of concentration of boron in graphene by PGAA

H. Ling Poh, P. Šimek, Z. Sofer, I. Tomandl and M. Pumera: *Boron and nitrogen doping graphene via thermal exfoliation of graphite oxide in a BF_3 or NH_3 atmosphere*
Journal of Materials Chemistry A: DOI: 10.1039/c3ta12460f

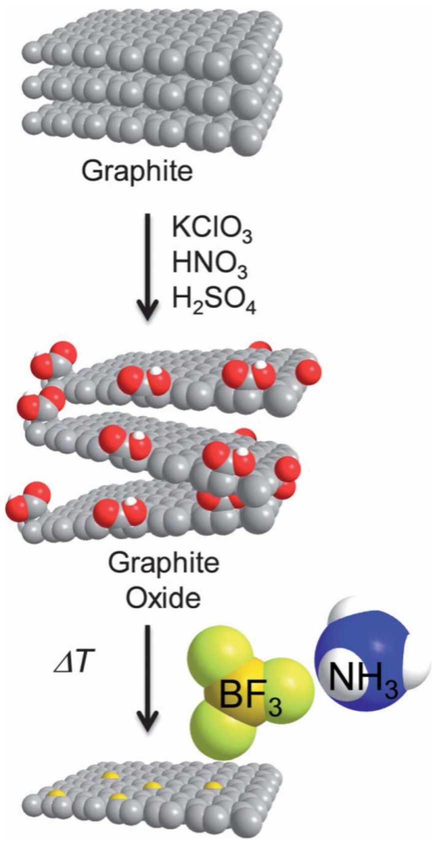

Fabrication of B and N doped graphenes by thermal exfoliation of graphite oxide prepared in BF_3 and NH_3 atmosphere.

Optical, electrical, mechanical and electrochemical properties of graphene can be modulated with heteroatoms

Proposed *scalable* method of implanting boron ("electron aceptor") and nitrogen ("electron donor") into graphene lattice

Boron concentration
in graphenes measured
at ***LWR-15 Rez*** by PGAA

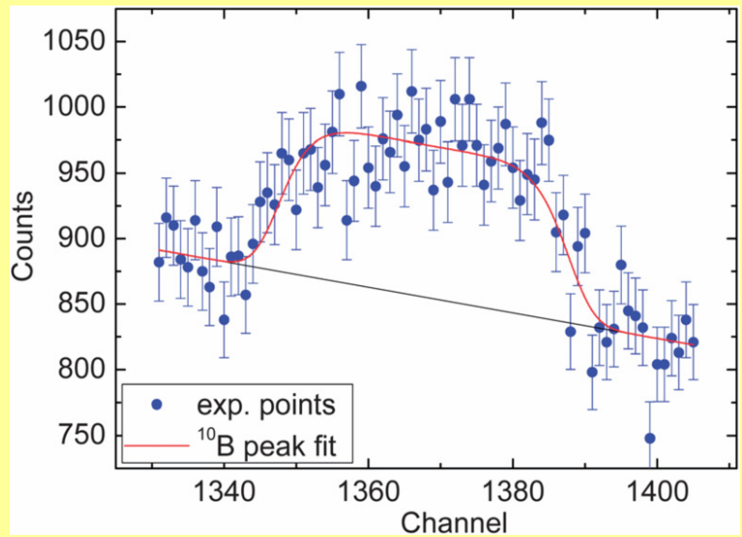

Part of PGAA spectrum containing Doppler broadened ^{10}B peak.

Other properties characterized by Raman spectroscopy and high-Resolution XPS

Summary

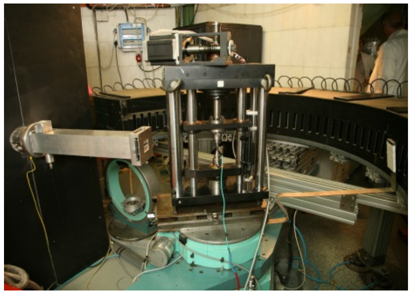

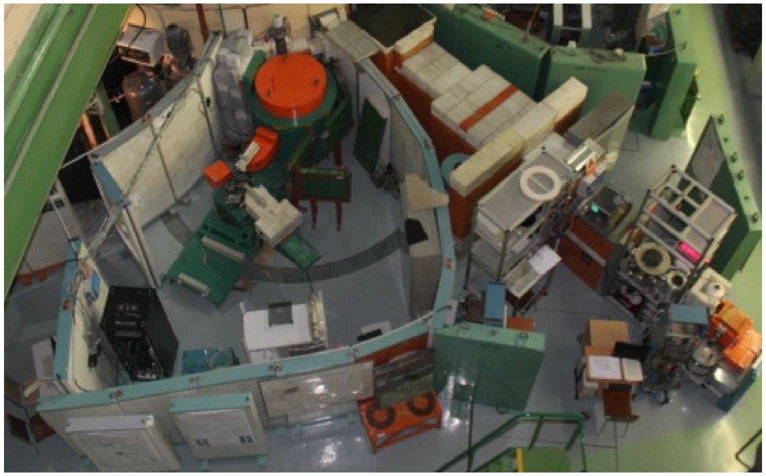

Open access

- continuous and fast evaluation of proposals
- support from in-house scientists for external users
- eligible users from EU and associated states: support within NMI3 project

NMI3 (Integrated Infrastructure Initiative for Neutron Scattering and Muon Spectroscopy): European consortium of 18 partner organisations from 12 countries, including all major neutron-physics labs

Open access statistics since Sept. 2012 (≈ the start of user portal):

- **29** external NPL proposals accepted (**8** CZ, **21** from abroad)
- **17** experiments already finished (**178** beamdays)
- **≈30** scientific papers per year (NPL- incl. internal experiments)

Conclusion

It can be stated that a large variety of competetive experi-ments of basic, interdisciplinary and applied research can be carried out at the medium power research reactors. Low and medium power neutron sources offer excellent oportunity for education and training of young scientists.